Structural Engineering and Mechanics, Vol. 3, No. 3 (1995) 289-297
DOI: http://dx.doi.org/10.12989/sem.1995.3.3.289

A finite element algorithm for contact problems with friction

C.H. Liu†, G. Hofstetter‡ and H.A. Mang‡

Institute for Strength of Materials, Technical University of Vienna, Karlsplatz 13, A-1040 Vienna, Austria

Abstract. A finite element algorithm for consideration of contact constraints is presented. It is characterized by introducing the geometric constraints, resulting from contact conditions, directly into the algebraic system of equations for the incremental displacements of an incremental iterative solution procedure. The usefulness of the proposed algorithm for efficient solutions of contact problems involving large displacements and large strains is demonstrated in the numerical investigation.

Key words: finite elements; contact problem; friction, geometric constraints; large displacements; large strains.

1. Introduction

Within the framework of the finite element method formulations for problems involving contact constraints can be classified into constraint minimization formulations (Lagrange multiplier method (Hughes, *et al.* 1976, Bathe and Chaudhary 1985, Chaudhary and Bathe 1986), penalty method (Kikuchi and Oden 1984, Oden and Pires 1984, Peric and Owen 1992, Papadopoulos and Taylor 1992), perturbed Lagrangian method (Ju and Taylor 1988, Simo, *et al.* 1985, Chang, *et al.* 1987), augmented Lagrangian method (Landers and Taylor 1985, Simo and Laursen 1992, Wriggers and Zavarise 1993)) and methods, characterized by imposing the geometric constraints resulting from contact directly on the equilibrium configuration (Chandrasekaran, *et al.* 1987). For an extensive list of references we refer to Zhong and Mackerle (1992).

In what follows, a relatively simple yet efficient method for the solution of contact problems at finite strains, taking into account friction in the contact zone, is presented. The proposed algorithm is characterized by directly enforcing the displacement constraints, resulting from the contact conditions, in the algebraic system of equations for the nodal incremental displacements. Advantages of the proposed algorithm are its simplicity, the exact enforcement of contact constraints, a well-conditioned stiffness matrix and even a small reduction of the number of the degrees of freedom in consequence of the constraints. In the numerical investigations, comparisons with numerical solutions in the literature are included, which demonstrate the efficiency of the proposed algorithm.

2. Formulation of the algorithm

Within the framework of an incremental-iterative finite element formulation the equilibrium

† Post-Doc Student
‡ Professor

configurations of two bodies B^1 and B^2 are assumed to be known up to load step n. Thus, the displacement field of the two bodies $\boldsymbol{u}_n=[\boldsymbol{u}_n^1:\boldsymbol{u}_n^2]^T$ is known. The algebraic system of equations for the vector of incremental nodal displacements, $\Delta\boldsymbol{u}_{n+1}=[\Delta\boldsymbol{u}_{n+1}^1:\Delta\boldsymbol{u}_{n+1}^2]^T$, for load step $n+1$, resulting from the linearized principle of virtual displacements, is given as

$$\boldsymbol{K}_n\Delta\boldsymbol{u}_{n+1}=\Delta\boldsymbol{F}_{n+1} \tag{1}$$

In Eq. (1) $\boldsymbol{K}_n$ denotes the tangent stiffness matrix at the known configuration, depending on the displacements $\boldsymbol{u}_n$; $\Delta\boldsymbol{F}_{n+1}$ is the vector of incremental nodal forces for load step $n+1$. Obviously, because of the linearization on which Eq. (1) is based, $\Delta\boldsymbol{u}_{n+1}$ is an approximation to the incremental displacements for load step $n+1$. Hence, an iterative technique has to be employed for each load increment to obtain the solution of the respective nonlinear problem. To this end, Eq. (1) is replaced by

$$\boldsymbol{K}_{n+1}^{(p-1)}\Delta\boldsymbol{u}_{n+1}^{(p)}=\boldsymbol{R}_{n+1}^{(p)}, \tag{2}$$

where p denotes an iteration step within load step $n+1$ and $\boldsymbol{R}_{n+1}^{(p)}$ stands for the vector of residual nodal forces. For $p=1$, $\boldsymbol{K}_{n+1}^{(0)}\equiv\boldsymbol{K}_n$ and $\boldsymbol{R}_{n+1}^{(1)}\equiv\Delta\boldsymbol{F}_{n+1}$. Consequently, the total displacements are obtained as

$$\boldsymbol{u}_{n+1}^{(p)}=\boldsymbol{u}_n+\sum_{i=1}^{p}\Delta\boldsymbol{u}_{n+1}^{(i)} \tag{3}$$

Fig. 1 shows those parts of two deformable bodies B^1 and B^2, which, upon examination of the displacement field $\boldsymbol{u}_{n+1}^{(p)}$ have come into contact. The bodies are discretized by means of isoparametric finite elements. For simplicity the subsequent derivations are restricted to two-dimensional problems. In what follows the subscript $n+1$ for the load increment and the superscript p for the iteration step will be omitted. The applied contact kinematics are based on the condition to prevent a penetration of body B^2 into body B^1. As can be seen from Fig. 1, this condition is violated by node s of body B^2. The normal projection of node s of body B^2 to the boundary of body B^1 yields point k. According to the isoparametric concept, the position vector $\boldsymbol{x}_k$ referred to body B^1 is given as

$$\boldsymbol{x}_k=\sum_{j=1}^{m}\boldsymbol{N}_j^e(\xi)\boldsymbol{x}_j^e, \tag{4}$$

where $\boldsymbol{N}_j^e$ and $\boldsymbol{x}_j^e$ denote matrices of suitable shape functions and the vectors of nodal coordinates in the current configuration of element e and ξ is a local coordinate which will be defined

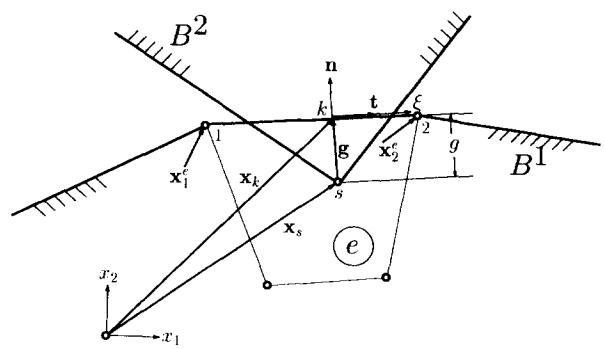

Fig. 1 Contact kinematics.

in the following. In Eq. (4) the summation extends over those m nodes of element e, which are located on the contact surface. The tangent vector $\boldsymbol{t}$ and the normal vector $\boldsymbol{n}$ to the boundary of element e at point k are given as

$$\boldsymbol{t}=\sum_{j=1}^{m}\frac{\partial N_j^e}{\partial \xi}\boldsymbol{x}_j^e \quad \text{and} \quad \boldsymbol{n}=\begin{bmatrix}0 & 1\\ -1 & 0\end{bmatrix}\frac{\boldsymbol{t}}{|\boldsymbol{t}|}, \tag{5}$$

respectively. ξ is computed from the condition

$$\boldsymbol{t}\cdot\boldsymbol{g}=0,\ \boldsymbol{g}=\boldsymbol{x}_k-\boldsymbol{x}_s \tag{6}$$

yielding, e.g., for a bilinear 4-node element

$$\xi=\frac{2\boldsymbol{a}\cdot(\boldsymbol{x}_s-\boldsymbol{x}_1^e)}{\boldsymbol{a}\cdot\boldsymbol{a}}-1 \tag{7}$$

with $\boldsymbol{a}=\boldsymbol{x}_2^e-\boldsymbol{x}_1^e$. For quadratic elements Eq. (6) can be solved by an iterative technique. The penetration g of node s into element e is obtained as

$$g=\boldsymbol{n}\cdot\boldsymbol{g} \tag{8}$$

Hence, if $g>0$, then the contact constraint will be violated (see Fig.1). Consequently, geometric compatibility has to be restored in the subsequent iteration step.

For sticking contact, the position of node s is assumed to be at point k on the boundary of element e. Hence, for the subsequent iteration step the condition

$$\boldsymbol{x}_s=\boldsymbol{x}_k \tag{9}$$

holds, where

$$\boldsymbol{x}_i=\bar{\boldsymbol{x}}_i+\Delta\boldsymbol{u}_i, \tag{10}$$

with $\bar{\boldsymbol{x}}_i$ as the known position vector from the previous iteration step. Substitution of Eq. (10) into Eq. (9) and use of $\Delta\boldsymbol{u}_k=\Sigma_{j=1}^{m}N_j^e(\xi)\Delta\boldsymbol{u}_j^e$, following on the basis of the isoparametric concept from Eq. (4), yields

$$\Delta\boldsymbol{u}_s=\sum_{j=1}^{m}N_j^e(\xi)\Delta\boldsymbol{u}_j^e+\boldsymbol{g} \tag{11}$$

In a local coordinate system, defined by the axes $\boldsymbol{t}$ and $\boldsymbol{n}$ at point k, the component of $\boldsymbol{g}=\bar{\boldsymbol{x}}_k-\bar{\boldsymbol{x}}_s$ in the directions of $\boldsymbol{t}$ and $\boldsymbol{n}$ are given as 0 and $\bar{g}=|\boldsymbol{g}|$, respectively. Hence, by means of a suitable transformation matrix $\boldsymbol{A}$ the relation between the local and the global coordinate system is obtained as

$$\boldsymbol{g}=\boldsymbol{A}\begin{Bmatrix}0\\ \bar{g}\end{Bmatrix}, \tag{12}$$

For sliding contact, Eq. (12) is replaced by

$$\boldsymbol{g}=\boldsymbol{A}\begin{Bmatrix}\Delta u_t\\ \bar{g}\end{Bmatrix}, \tag{13}$$

where Δu_t denotes the unknown displacement component of node s, in the tangential direction to the boundary of element e at node k.

Note that modelling of sticking contact in this way involves an inaccuracy, because the assumed

position of node s at point k is not necessarily the point, where node s touches the boundary of element e.

Making use of Eq. (11), the global vector of nodal displacement increments $\Delta \boldsymbol{u}$ can be rewritten as

$$\Delta \boldsymbol{u}=\begin{Bmatrix} \Delta \boldsymbol{u}_1 \\ \vdots \\ \Delta \boldsymbol{u}_1^e \\ \Delta \boldsymbol{u}_2^e \\ \vdots \\ \Delta \boldsymbol{u}_n^e \\ \vdots \\ \Delta \boldsymbol{u}_s \\ \vdots \end{Bmatrix} = \begin{bmatrix} 1 & & & & & & & \\ & \ddots & & & & & & \\ & & 1 & & & & & \\ & & & 1 & & & & \\ & & & & \ddots & & & \\ & & & & & 1 & & \\ & & & & & & \ddots & \\ & & & N_1^e\, N_2^e & \cdots & N_n^e & \cdots & \boldsymbol{A} \\ & & & & & & & \ddots \end{bmatrix} \begin{Bmatrix} \Delta \boldsymbol{u}_1 \\ \vdots \\ \Delta \boldsymbol{u}_1^e \\ \Delta \boldsymbol{u}_2^e \\ \vdots \\ \Delta \boldsymbol{u}_n^e \\ \vdots \\ g \\ \vdots \end{Bmatrix} = \boldsymbol{C}_{s1}\, \Delta \boldsymbol{u}_{s1}. \tag{14}$$

Application of Eq. (14) to all nodes of body B^2, which have penetrated into B^1 in the previous iteration step, by replacing the subscript s_1 in Eq. (14) consecutively by s_2, s_3, $\cdots$, s_l, where l denotes the number of nodes with active contact constraints, yields

$$\Delta \boldsymbol{u}=\boldsymbol{C}_{s1}\,\Delta \boldsymbol{u}_{s1}=\boldsymbol{C}_{s1}\boldsymbol{C}_{s2}\,\Delta \boldsymbol{u}_{s2}=\cdots=\boldsymbol{C}_{s1}\boldsymbol{C}_{s2}\cdots\boldsymbol{C}_{sl}\,\Delta \boldsymbol{u}_{sl}=\boldsymbol{C}\,\Delta \boldsymbol{u}_{sl}, \tag{15}$$

with

$$\boldsymbol{C}=\boldsymbol{C}_{s1}\boldsymbol{C}_{s2}\cdots\boldsymbol{C}_{sl}. \tag{16}$$

Substitution of Eq. (15) into Eq. (2) and pre-multiplication of the resulting system of equations by $\boldsymbol{C}^T$ yields

$$\boldsymbol{C}^T\boldsymbol{K}\boldsymbol{C}\,\Delta \boldsymbol{u}_{sl}=\boldsymbol{C}^T\boldsymbol{R}. \tag{17}$$

Because of the time-consuming matrix multiplications involved in Eq. (16) and in Eq. (17) and the memory requirements for the matrix $\boldsymbol{C}$ at a first sight the proposed algorithm seems to be inefficient. However, in practice, the matrix $\boldsymbol{C}$ as well as the matrices $\boldsymbol{C}_{si}$ ($i=1, \cdots, l$) are not computed explicitly. Rather, $\boldsymbol{C}^T\boldsymbol{K}\boldsymbol{C}$ and $\boldsymbol{C}^T\boldsymbol{R}$ are computed by employing the recursive scheme

$$^{(1)}\boldsymbol{K}=\boldsymbol{C}_{s1}^T\,{}^{(0)}\boldsymbol{K}\boldsymbol{C}_{s1} \qquad {}^{(1)}\boldsymbol{R}=\boldsymbol{C}_{s1}^T\,{}^{(0)}\boldsymbol{R}, \tag{18}$$

$$^{(2)}\boldsymbol{K}=\boldsymbol{C}_{s2}^T\,{}^{(1)}\boldsymbol{K}\boldsymbol{C}_{s2} \qquad {}^{(2)}\boldsymbol{R}=\boldsymbol{C}_{s2}^T\,{}^{(1)}\boldsymbol{R}, \tag{19}$$

$$^{(i)}\boldsymbol{K}=\boldsymbol{C}_{si}^T\,{}^{(i-1)}\boldsymbol{K}\boldsymbol{C}_{si} \qquad {}^{(i)}\boldsymbol{R}=\boldsymbol{C}_{si}^T\,{}^{(i-1)}\boldsymbol{R}, \text{ for } i=3, \cdots, l, \tag{20}$$

where ${}^{(0)}\boldsymbol{K}=\boldsymbol{K}$, ${}^{(0)}\boldsymbol{R}=\boldsymbol{R}$ and, finally, ${}^{(l)}\boldsymbol{K}=\boldsymbol{C}^T\boldsymbol{K}\boldsymbol{C}$, ${}^{(l)}\boldsymbol{R}=\boldsymbol{C}^T\boldsymbol{R}$.

Note that the vector $\Delta \boldsymbol{u}_{sl}$ contains both, unknown and prescribed nodal displacements. The latter result from the contact constraints. For the prescribed nodal displacements the corresponding nodal reaction forces converge to the nodal contact forces. Transformation of the reaction forces at node s into components parallel to $\boldsymbol{t}$ and $\boldsymbol{n}$ yields the tangential component f_t and the normal component f_n. The pressure in the contact zone is computed according to Bathe and Chaudhary (1985). According to Coulomb's law, sticking occurs, if $|f_t|<\mu|f_n|$, where μ denotes the coefficient of friction. Otherwise sliding is assumed. For sliding, because of the absence of a constraint in tangential direction, the respective component f_t of the reaction force will converge to zero, representing frictionless sliding. Frictional sliding, however, is characterized by a non-zero tangential component of the reaction force. For this reason a set of equilibrium forces is added, consisting

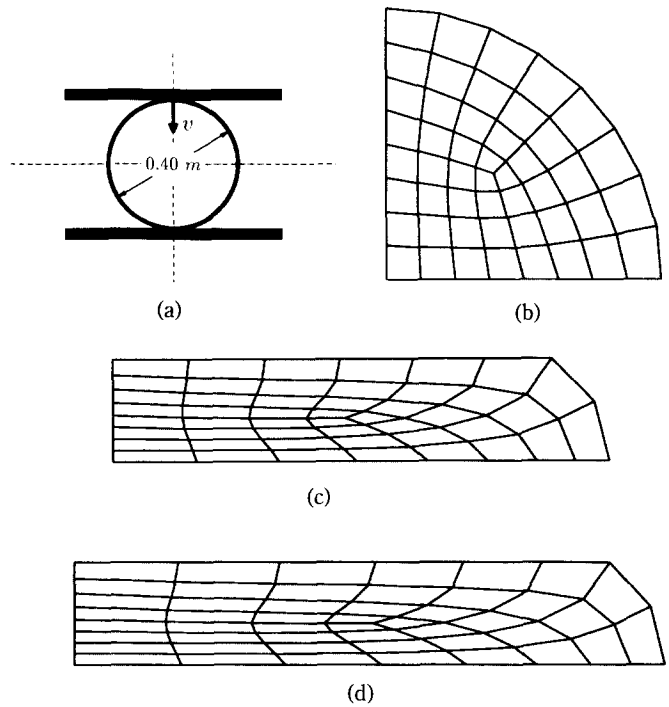

Fig. 2 Rubber cylinder, squeezed between two rigid plates
(a) Cross section; (b) FE-mesh; (c) Deformed structure ($K=11.28$ MPa); (d) Deformed structure ($K=1410$ MPa).

of $f_t=\mu f_n$, applied at node s. This set of forces is balanced by forces of equal magnitude, but acting in the opposite direction, applied at the nodes of element e as work equivalent nodal forces.

3. Numerical examples

The proposed contact algorithm is tested for contact problems involving either a deformable body and a rigid body or two deformable bodies. In both cases large displacements and large strains are taken into account.

The first example is characterized by the squeezing of a rubber cylinder between two rigid, frictionless plates, assuming plane strain conditions (Fig. 2(a)). This is a standard example to test contact algorithms (Simo and Taylor 1991, Sussman and Bathe 1987). The diameter of the cylinder is 0.40 m, the material parameters of the Mooney-Rivlin material model are given as $C_1=0.293$ MPa and $C_2=0.177$ MPa, respectively. The bulk modulus K is 1410 MPa. Hence, because of $G=2(C_1+C_2)$, the ratio of K over the shear modulus G is equal to 1500, yielding nearly incompressible material behavior. The FE-mesh of one quarter of the cylinder is shown in Fig. 2(b). Following Simo and Taylor (1991), a total relative displacement of the plates of $v=0.25$ m is applied in one step. The solution of the problem is split into two increments. In the first increment K is set to 11.28 MPa to avoid problems resulting from nearly incompressible

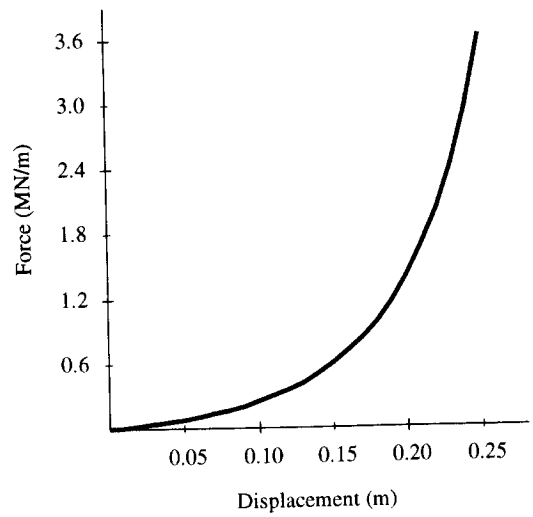

Fig. 3 Load-deflection diagram for the rubber cylinder, squeezed between two rigid plates.

material behavior. The respective deformed structure is shown in Fig. 2(c). In order to account for the nearly incompressible material behavior, in the second increment K is increased up to the final value of 1410 MPa, yielding the deformed structure, shown in Fig. 2(d). Altogether, 16 iteration steps are needed to obtain a value of the norm of the residual energy, which is less than $1 \cdot 10^{-11}$ MNm/m. Inspection of Fig. 2(d) and of the respective figure in Simo and Taylor (1991) reveals excellent agreement of the computed deformed configuration. The load-deflection diagram for this example is shown in Fig. 3. Up to a total deflection of 0.2 m it can be compared with the respective diagram, contained in Sussman and Bathe (1987). In this reference a total displacement of 0.2 m was applied in 10 equal steps. For this range of deflection the two load-deflection curves are identical. The vertical load, corresponding to the deflection of 0.2 m, is equal to 1.40 MN/m. The vertical load, corresponding to the final deflection of 0.25 m, shown in Fig. 2(d), is equal to 3.64 MN/m.

The second example is dealing with a cylindrical ring, squeezed between two elastic plates (Fig. 4(a)). This example has been solved in Papadopoulos and Taylor (1992) on the basis of a mixed penalty formulation, neglecting friction between the ring and the plates, and in Wriggers and Zavarise (1993), employing a nonlinear contact law within the framework of an augmented Lagrangian technique. Following Papadopoulos and Taylor (1992), the geometric and material parameters are chosen without referring to particular physical dimensions. A uniform vertical displacement v is applied to the top surface of the upper plate. In Papadopoulos and Taylor (1992) this problem has been analyzed up to $v=4$. Because of symmetry conditions, only one quarter of the structure needs to be discretized (Fig. 4(b)). (In Papadopoulos and Taylor (1992) and Wriggers and Zavarise (1993) the results are referred to one half of the value of the prescribed displacement v, applied on the horizontal symmetry plane of the ring.)

The ring and the plates are assumed to be made of materials, obeying Neo-Hookean constitutive relations. For the former, the bulk modulus and the shear modulus are chosen as $K=833$ and $G=385$, respectively, for the latter $K=83300$ and $G=38500$, respectively.

Firstly, frictionless contact is considered. A displacement of $v=8$ is applied in 4 equal increments. Fig. 4(c) and Fig. 4(d) show the deformed structure, corresponding to $v=4$ and $v=8$, respectively. In Fig. 5 the pressure distributions in the contact surface are plotted for several

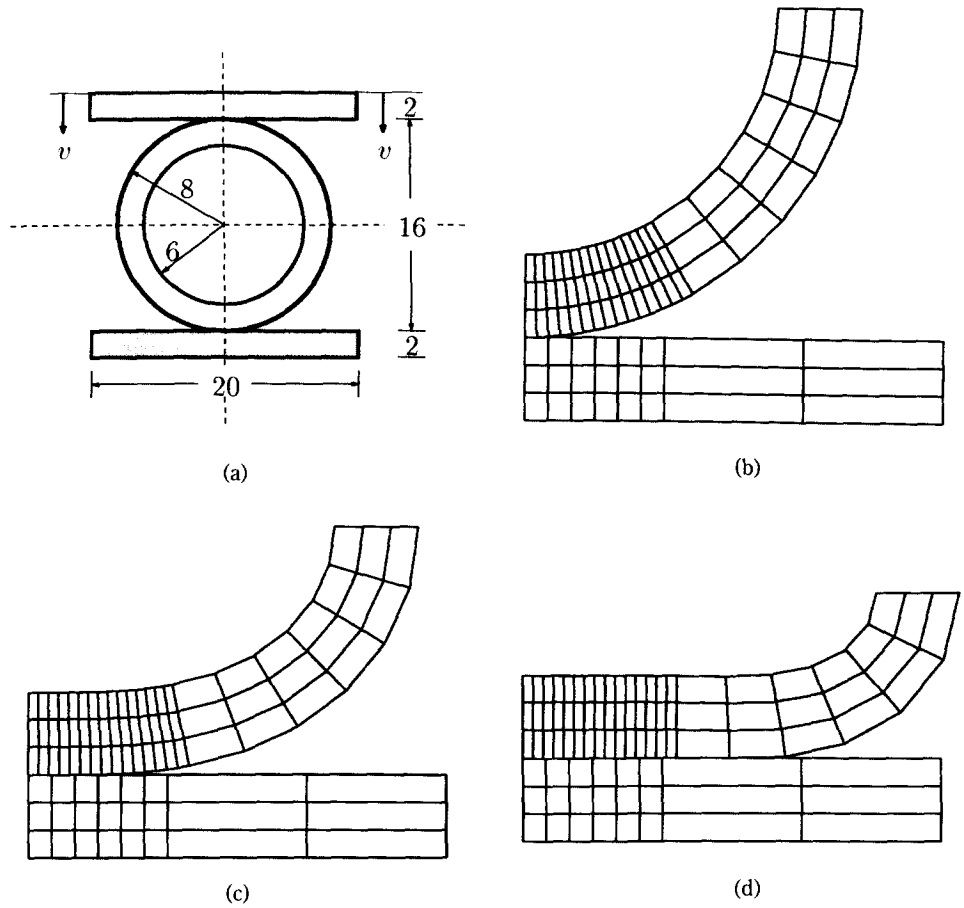

Fig. 4 Cylindrical ring, squeezed between two elastic plates
(a) Cross section; (b) FE-mesh; (c) Deformed structure ($v=4$); (d) Deformed structure ($v=8$).

levels of v. For $v=2$ and $v=4$ the pressure distributions in the contact region can be compared with the results reported in Papadopoulos and Taylor (1992). The length of the contact region, the peak pressure in the vertical symmetry plane as well as the distribution of the pressure in the contact region are in good agreement with the results contained in Papadopoulos and Taylor (1992).

For vertical deflections larger than $v=4$ Fig. 5 shows a decrease of the contact pressure in the region close to the vertical symmetry plane until, finally, the contact pressure is reduced to zero in this region, indicating tension release. Remarkably, quite large displacement increments may be chosen. Even application of the total displacement of $v=8$ in one single step yields convergence within 11 iteration steps. The convergence tolerance is chosen in terms of the norm of the residual forces to be less than $1 \cdot 10^{-6}$ MN/m. In Wriggers and Zavarise (1993) this example was analyzed up to a vertical deflection of $v=6$, taking into account a nonlinear constitutive law in the contact interface. In spite of this difference a similar qualitative behavior in the contact region is observed.

Secondly, frictional contact is investigated, assuming the coefficient of friction μ to be equal to 0.2 and 0.4, respectively. Compared with frictionless conditions, the displacement steps have

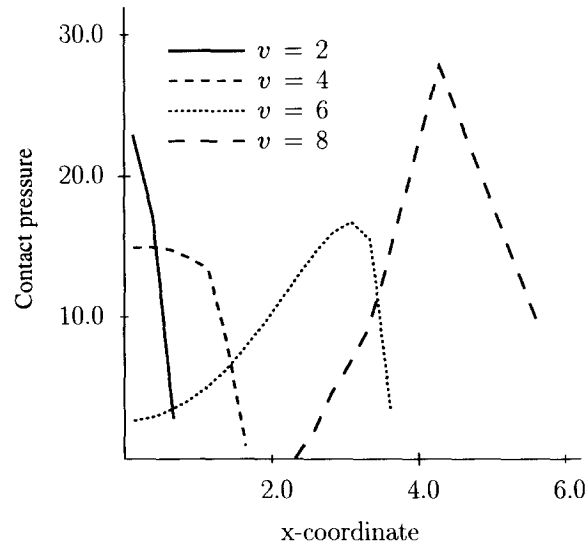

Fig. 5 Pressure distribution in the contact surface for different values of v.

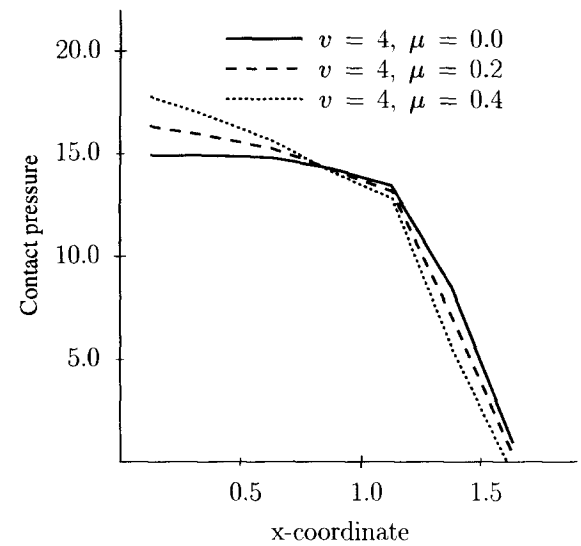

Fig. 6 Comparison of the pressure distribution in the contact surface for different values of μ.

to be chosen considerably smaller in order to properly account for the path-dependence of such problems. In particular, a total vertical displacement of $v=4$ is applied in 20 equal steps. A comparison of the pressure distributions in the contact surface for different values of μ at $v=4$ is contained in Fig. 6.

4. Conclusions

On the basis of the proposed finite element algorithm for contact problems the geometric constraints, resulting from contact conditions, are accounted for directly in the algebraic system

of equations for the incremental displacements in the context of an incremental-iterative solution procedure. An advantage of the proposed algorithm is its conceptual simplicity. Nevertheless, the introduction of constraints into the global system of equations may prove to be difficult in large FE-codes. In the numerical study it was shown that the proposed algorithm is capable of efficiently solving contact problems, involving large displacements and large strains.

References

Bathe, K.J. and Chaudhary, A. (1985), "A solution method for planar and axisymmetric contact problems", *Int. J. Numer. Meth. Engng.*, **21**, 65-88.

Chandrasekaran, N., Haisler, W.E. and Goforth, R.E. (1987), "A finite element solution method for contact problems with friction", *Int. J. Numer. Meth. Engng.*, **24**, 477-495.

Chang, T.Y., Saleeb, A.F. and Shyu, S.C. (1987), "Finite element solution of two-dimensional contact problems based on a consistent mixed formulation", *Comput. Struct.*, **27**, 455-466.

Chaudhary, A. and Bathe, K. J. (1986), "A solution method for static and dynamic analysis of three-dimensional contact problems with friction", *Comput. Struct.*, **24**, 885-873.

Hughes, T. J. R., Taylor, R. L., Sackman, J. L., Curnier, A. and Kanoknukulchai, W. (1976), "A finite element method for a class of contact-impact problems", *Comput. Meth. Appl. Mech. Engng*, **8**, 249-276.

Ju, J. W. and Taylor, R. L. (1988), "A perturbed Lagrangian formulation for the finite element solution of nonlinear frictional contact problems", *J. Theor. Appl. Mech.*, Special Issue, **7**, 1-14.

Kikuchi, N. and Oden, J. T. (1984), "Contact problem in elasto-statics", in *Finite Elements*, **5**, Eds. Oden, J. T. and Carey, G. F., Prentice-Hall, Englewood Cliffs, NJ.

Landers, J. A. and Taylor, R. L. (1985), "An augmented Lagrangian formulation for the finite element solution of contact problems", *Report No. UCB/SESM-85/09*, University of California Berkeley.

Oden, J. T. and Pires, E. B. (1984), "Algorithms and numerical results for finite element approximations of contact problems with non-classical friction laws", *Comput. Struct.*, **19**, 137-147.

Papadopoulos, P. and Taylor, R. L. (1992), "A mixed formulation for the finite element solution of contact problems", *Comp. Meth. Appl. Mech. Engr.*, **94**, 373-389.

Perić, D. and Owen, D. R. J. (1992), "Computational model for 3-D contact problems with friction based on the penalty method", *Int. J. Numer. Meth. Engng.*, **35**, 1289-1309.

Simo, J. C., Wriggers, P. and Taylor, R. L. (1985), "A perturbed Lagrangian formulation for the finite element solution of contact problems", *Comput. Meth. Appl. Mech. Engng.*, **50**, 163-180.

Simo, J. C. and Taylor, R. L. (1991), "Quasi-incompressible finite elasticity in principal stretches, continuum basis and numerical algorithms", *Comp. Meth. Appl. Mech. Engr.*, **85**, 273-310.

Simo, J. C. and Laursen, T. A. (1992), "An augmented Lagrangian treatment of contact problems involving friction", *Comput. Struct.*, **42**, 97-116.

Sussman, T. and Bathe, K. J. (1987), "A finite element formulation for nonlinear incompressible elastic and inelastic analysis", *Comp. Struct.*, **26**(1/2), 357-409.

Wriggers, P. and Zavarise, G. (1993), "Application of augmented Lagrangian techniques for non-linear constitutive laws in contact interfaces", *Comm. Num. Meth. Eng.*, **9**, 815-824.

Zhong, Z. H. and Mackerle, J. (1992), "Static contact problems-A review", *Engineering Computations*, **9**, 3-37.